ELSEVIER

Chemical Engineering Journal 123 (2006) 93–102

Chemical Engineering Journal

www.elsevier.com/locate/cej

Catalyst preparation for fabrication of a MEMS fuel reformer

Taegyu Kim, Sejin Kwon *

Division of Aerospace Engineering, Korea Advanced Institute of Science and Technology, 373-1 Guseong-dong, Yuseong-gu, Daejeon 305-701, Republic of Korea

Received 13 March 2006; received in revised form 31 July 2006; accepted 1 August 2006

Abstract

Fabrication procedures for a micro fuel reformer including catalyst preparation, coating, and patterning on a wafer are described. Cu/ZnO catalyst was selected for the steam reforming of methanol. The catalysts were prepared by three different procedures according to the precipitation sequence and temperature. The effect of precipitation conditions on the catalyst characteristics was investigated by BET, XRD and SEM analysis. Catalytic activity and coating quality were tested to find the optimum precipitation condition for the uniform and crack-free catalyst layer on a wafer. For coating purpose, the prepared catalyst was ground by ball-mill into powder and mixed with binder in the deionized water. Simultaneous precipitation of catalyst and binder on the wafer produced a catalyst layer that is uniform and rigidly found to the wafer surface. The amount of the coated catalyst was 5–8 mg/cm^2 and the thickness was 30 μm. By repetition of the coating procedure, the catalyst mass up to 15 mg/cm^2 was obtained with increased reactivity. Patterned catalyst layer was obtained by a novel lift-off process of the PVA sacrificial layer. The process consists of the PVA decomposition by heating instead of etching the wafer. A micro fuel reformer was fabricated using a typical lithography procedure including catalyst coating and patterning process and its performance was measured. The catalyst-coated micro fuel reformer had higher performances than the packed-bed reactor.

Keywords: Coating; Patterning; Cu/ZnO catalyst; Micro fuel reformer; Methanol; Fuel cell

1. Introduction

Micro scale power sources with energy density that exceeds that of an existing secondary battery would find applications in diverse fields. Micro fuel cells have been a major candidate for a micro scale power source [1–12]. Direct methanol fuel cell (DMFC) has been widely investigated as a possible candidate for a micro power generation [10–12], but its output level is severely limited due to the problem of fuel cross over [12]. Polymer electrolyte membrane fuel cell (PEMFC) produces higher output with better efficiency than DMFC [13]. Gaseous hydrogen that fuels PEMFC takes too much volume to be contained in a micro scale device. Therefore, a fuel reformer that produces hydrogen from a liquid fuel is essential for development of a micro fuel cell system [14–22].

Among liquid fuels that are used for the fuel reforming in conventional scale devices, methanol is better suited for a micro scale reformer, as efficient reforming takes place at relatively low temperature [21–23]. Level of CO emission that poisons the PEMFC anode electrocatalyst [24] is lower with methanol as a fuel.

The Cu/ZnO-based catalyst is used for the production of hydrogen from methanol by steam reforming. The well-known catalyst is Cu/ZnO/Al_2O_3 [29–30]. Generally, it has been claimed that Cu^0 provides the catalytic activity and ZnO acts by stabilizing the Cu surface area. Addition of Al_2O_3 to the binary mixture enhances the Cu dispersion and catalyst stability [25]. Various methods for the preparation of Cu/ZnO-based catalysts have been reported. Co-precipitation is a typical method as a wet chemical process [26].

In many operations, the level of heat transfer to a reactor is the limiting condition for the conversion rate. When the reactor wall is coated with the catalyst, the catalyst layer will absorb more heats than the catalyst grains packed into the reactor volume. The catalyst, coated on the internal surface of the reactor, provides better retainment within the reactor bed than the granular catalyst packed inside the reactor [27].

For the development of a MEMS-based catalytic reactor for the fuel reforming [19–20], the patterning of the catalyst layer is key technology. Typical micro scale reactor uses the metal

---

* Corresponding author. Tel.: +82 42 869 3721; fax: +82 42 869 3710.
E-mail address: trumpet@kaist.ac.kr (S. Kwon).

1385-8947/$ – see front matter © 2006 Elsevier B.V. All rights reserved.
doi:10.1016/j.cej.2006.08.010

layer that is compatible to complementary metal oxide semiconductor (CMOS) metal deposition processes and the material is limited to the metal layer such as Pt. However, the technology on the patterning of catalyst particles prepared by co-precipitation is not established yet. E-beam lithography and other methods are on development for the patterning of nano particles [28].

In the present study, an optimum precipitation condition of Cu/ZnO catalyst is sought in the co-precipitation method that produces a good coating quality. The effect of temperature and sequence of the precipitation, in particulate, was closely monitored for better coating characteristics. In addition to catalyst coating, the patterning of the coated catalyst layer for a MEMS compatible process is essential in order to integrate the catalyst coating and lithographic fabrication process. For a patterning procedure, poly-vinyl alcohol (PVA) was selected as a sacrificial layer. Lift-off process of the PVA by heating was attempted. Combination of conditions that produce the best result was sought by changing the PVA concentration, viscosity of catalyst slurry, and catalyst thickness. A micro fuel reformer was fabricated by a typical lithography procedure that incorporates catalyst coating and patterning process developed in the present study and its performance for the steam reforming of methanol was tested.

2. Catalysts

2.1. Preparation

Briefly outlining, the preparation of the Cu/ZnO catalyst consists of the co-precipitation of Cu and Zn nitrates with the solution of sodium carbonate as a precipitating agent [25]. A 1.8 M aqueous solution of Na_2CO_3 is added to a 0.7 M aqueous solution of $Cu(NO_3)_2$ and a 0.3 M aqueous solution of $Zn(NO_3)_2$ by vigorous stirring under nitrogen atmosphere. In a step of catalyst preparation, the effect of precipitation conditions on the grain size, surface area, reactivity, and coating quality were examined. From this experiment, a suitable precipitation condition can be determined to obtain good coating quality. Three sets of test condition based on the precipitation sequence and temperature were chosen for a comparative study for Cu/ZnO catalysts. Co-precipitation (CP) at the precipitation temperature of 30 and 80 °C and the sequential precipitation (SP) at the temperature of 80 °C are three test conditions of Table 1. The pH was kept at 7.0 during the precipitation process. The precipitates were washed and dried at 120 °C for 2 h, followed by calcination at 350 °C for 6 h.

Table 1
An overview of prepared Cu/ZnO catalysts and BET surface area

Catalysts	Precipitation		BET surface area (m^2/g)
	Method	Temperature (°C)	
CP30-27	CP	30	27.49
CP80-35	CP	80	35.66
SP80-33	SP	80	33.71

2.2. Characterization

The surface areas were measured by the method of Brunauer, Emmett and Teller (BET). Powder X-ray diffractometer (XRD) pattern of the prepared catalyst was recorded on a Rigaku D/MAX-IIIB X-ray diffractometer, scanning 2θ angles from 20° to 80° with scan speed of $2^\circ\,\text{min}^{-1}$. The catalyst gains were examined by scanning electron microscope (SEM) analysis, and its particle size and extent of agglomeration were measured.

2.3. Catalytic activity

The prepared catalyst was tested for the methanol conversion reactivity using a tubular reforming reactor. The inside diameter and length of the reactor were 5.3 and 28 mm, respectively. Fig. 1 shows the schematic diagram of the system for the steam reforming of methanol. Prepared catalyst in powder was packed inside the reactor and kept in place by a glass wool filter. Preset amount of methanol was supplied to the reactor by a precision syringe pump. Methanol and water were evaporated by a vaporizer and entered the reactor at 150 °C. The reactor was placed inside a furnace so that the reactor temperature can be controlled. Reaction products were analyzed by gas chromatography (agilent HP-6890) using argon as a carrier gas. Methanol conversion was measured with the feed rate and reactor temperature as parameters. The catalyst amount was 50 mg and the steam to carbon ratio (S/C) was 1.1 because higher S/C is not suitable to a micro fuel reformer [16]. Mixture feed rate of methanol and water was between 0.1 and 1.6 ml/h. Reactor temperature was varied from 150 to 350 °C.

3. Catalyst coating

3.1. Slurry preparation

Cu/ZnO catalysts prepared by the co-precipitation are in powder state. In order to coat the catalyst, the powdered catalyst was further ground by a ball-mill to improve the dispersion of catalyst particles. The Cu/ZnO catalyst was loaded into a 500 ml ball-mill jar with 5 mm alumina grinding balls. The milling was done for 25 h at 250 rpm. The slurry was prepared by adding and stirring ground catalyst and binder into deionized water. Bentonite was used as a binder. The ratio of catalyst to binder was 2.5 and the solid wt.% of the slurry was 7%.

3.2. Coating procedure on a wafer

First, the wafer surface was washed with 1:4 mixtures of the hydrogen peroxide and sulfuric acid for 5 min at room temperature. The surface was rinsed with the deionized water for 5 min and dried at 80 °C. This step was performed to remove organic materials from the surface as well as to increase the extent of hydroxylation on the wafer surface [27].

Different coating methods were tested including the spin coating and dip coating. Low viscosity of the catalyst slurry and the limitation in dispersion resulted in a poor coating quality.

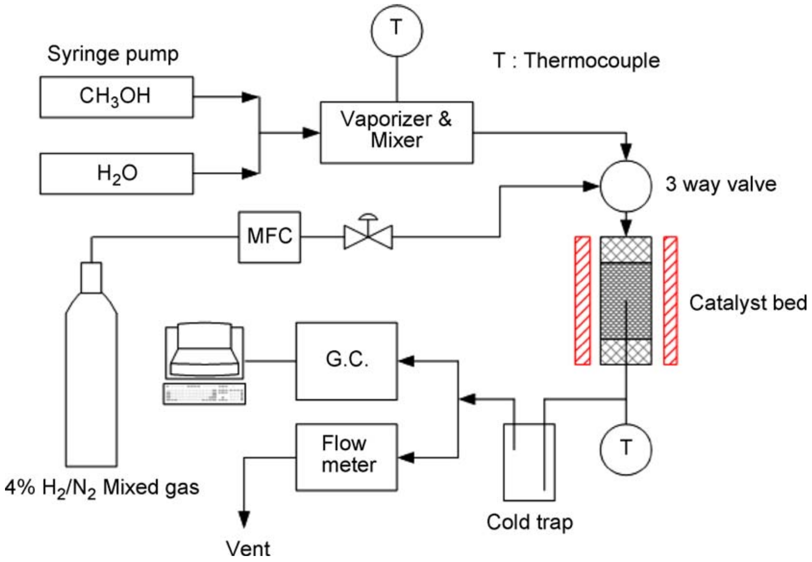

Fig. 1. Schematic diagram of the system for the steam reforming of methanol.

Simple powder precipitation technique, however, produced a satisfactory coating quality. In this method, the catalyst and binder were dispersed with water by sonication and stirring steps, and then the particles were precipitated on the top of the wafer as time goes on. After drying the water, the catalyst-coated wafer was fired at 500 °C, resulting in a good coating quality.

4. Catalyst patterning

4.1. PVA as a sacrificial layer

In order to integrate the catalyst coating procedure and conventional lithography process of a micro structure, a patterned coating is required. In a conventional micro fabrication of the metal patterning, PR (photo resist) or Poly-Si is used as a sacrificial layer. In case of the patterned catalyst, the sacrificial layer must withstand the high temperature and thermal stress that is caused by the firing process of the catalyst coating [28]. In the present study, a novel process for patterning catalyst on a wafer was introduced. PVA was used for a sacrificial layer. Deposited catalyst layer was patterned by the lift-off process of the PVA sacrificial layer.

4.2. Patterning procedure on a wafer

Overall patterning procedure is depicted in Fig. 2. First, 25% solution of PVA was prepared by dissolving PVA in deionized water at 70 °C. By spin coating of this solution, PVA layer was deposited on the wafer with PR (AZ6612) patterns (Fig. 2(4)). The thickness of PVA layer was controlled by the rotational frequency of spin coater. The ratio of PR to PVA was controlled into 3. When the PR pattern was removed, PVA pattern was left on the wafer surface (Fig. 2(5)). Then the catalyst was coated by the precipitation method on this substrate (Fig. 2(6)). A firing process of 500 °C, which is required for the calcination of the catalyst layer and for the interaction of catalyst and binder, removed PVA layer because the temperature of firing is higher than that of PVA thermal decomposition (Fig. 2(7)). PVA is decomposed rapidly at 300 °C.

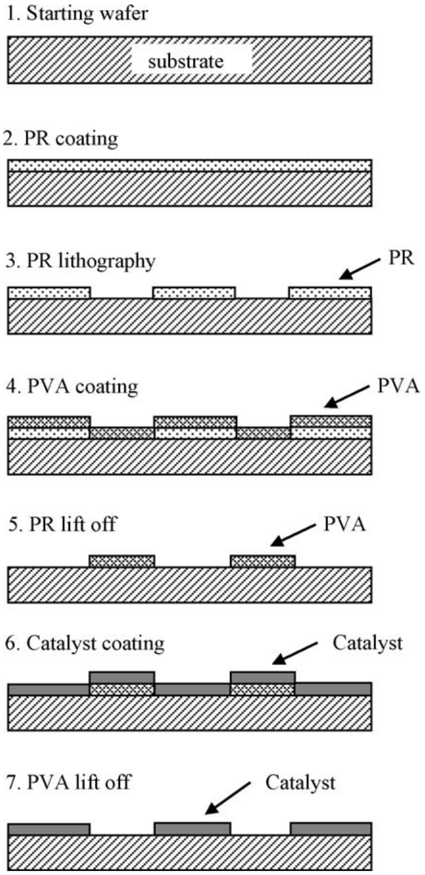

Fig. 2. Overall patterning procedure of the catalyst layer.

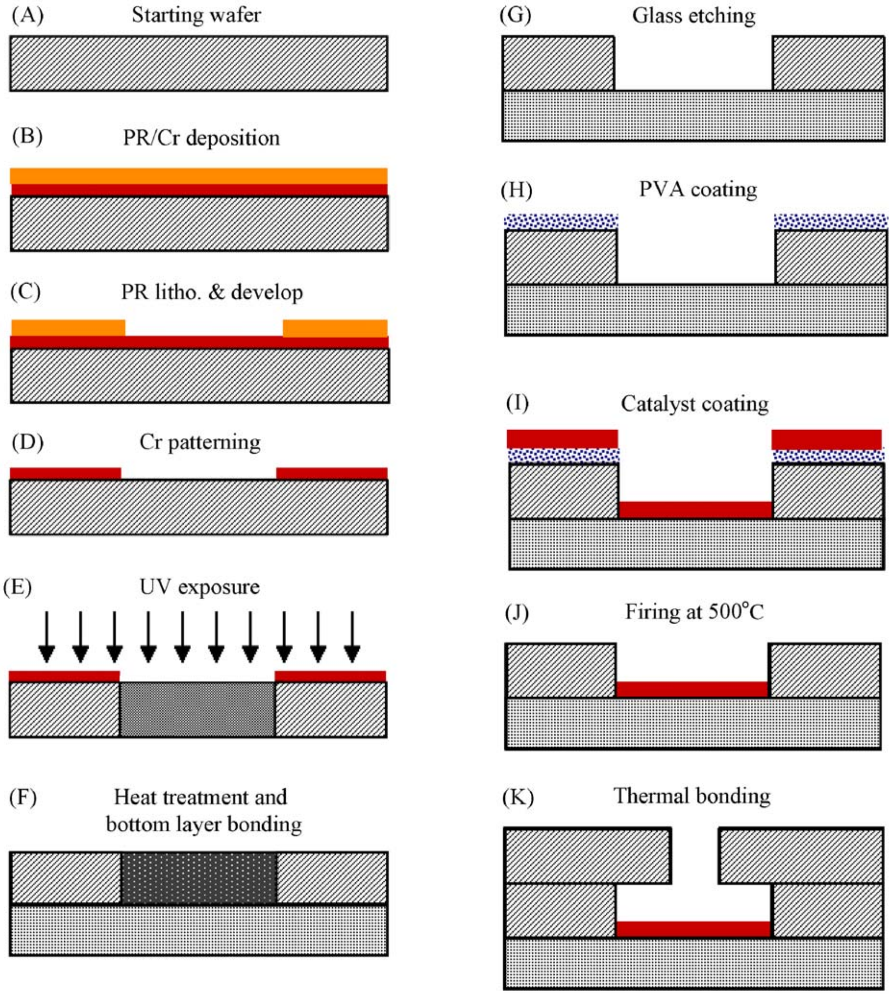

Fig. 3. Schematic of the fabrication process of a prototype micro fuel reformer; step A–G is wet anisotropic etching process for reactor structure, step H–J is coating and patterning process of catalyst layer, and lastly three layers is bonded at step K.

5. Fabrication of micro fuel reformer

A prototype micro fuel reformer was fabricated. A photoetchable glass wafer, Foturan® (made by Schott), was chosen as a structural material since the thermal insulation and gas sealing can be achieved easily with a material [31]. Fig. 3 depicts the overall fabrication procedure, which includes wet anisotropic etching of the photoetchable glass wafer (Fig. 3(A–G)), coating and patterning of catalyst layer on the wafer (Fig. 3(H–J)), and bonding of each layer (Fig. 3(K)). Structuring of the photoetchable glass wafer consists of chromium mask patterning (Fig. 3(A–D)), UV light exposure (Fig. 3(E)), heat treatment for crystallization (Fig. 3(F)), and hydrofluoric acid (HF) etching (Fig. 3(G)) [32]. Three wafer layers were fusion-bonded for a single reactor structure. Reactant entrance and product exit were fabricated on the top layer. Microchannel was engraved in the center layer and the catalyst was coated and patterned on the internal surface. Fig. 4 shows the completed device which is coated with the catalyst of 12 mg.

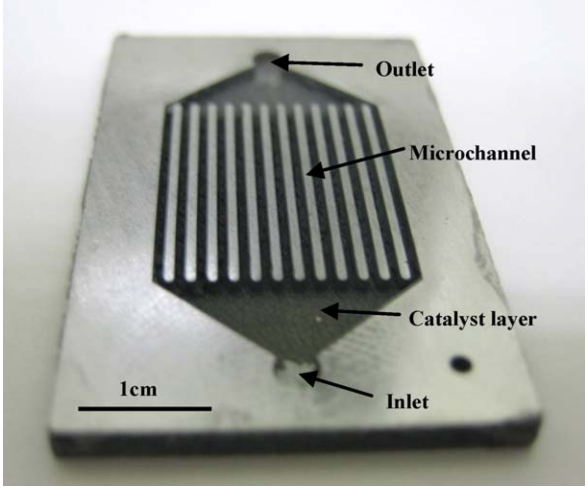

Fig. 4. The fabricated micro fuel reformer with the Cu/ZnO catalyst coated in the microchannel. The channel width is 500 μm, reactor chamber size is 1.5 cm × 2 cm × 0.1 cm.

6. Results and discussion

6.1. Effect of precipitation conditions on characteristics of Cu/ZnO catalysts

The results of BET measurement are included in Table 1. The surface area increased as the precipitation temperature increased from 30 to 80 °C within the same co-precipitation condition. Co- and sequential precipitation did not show much difference in the surface area when the precipitation temperature remains the same.

XRD patterns of Cu/ZnO catalysts after preparation were shown in Fig. 5. For all three catalysts prepared by different precipitation methods, Cu and Zn species in the catalysts mainly existed as metal oxides and no XRD peaks of species containing both Cu and Zn were observed. Intensity of XRD peaks changed with the precipitation method and temperature. Crystal structure of the catalyst prepared by CP at 30 °C was better defined than that of catalysts prepared by CP and SP at 80 °C. As known from XRD pattern of the catalyst prepared by SP at 80 °C, the Cu crystal was not observed well because the Zn addition during the Cu precipitation affected the crystallization of Cu.

Fig. 6 is SEM images of catalysts precipitated by the three conditions described in Table 1. Typical grain size of all catalysts ranged 20–50 nm. The individual catalyst grains were well defined in CP at 30 °C case. Catalyst grains in CP and SP at 80 °C coagulated into larger lumps than that of in CP at 30 °C. This is caused by the difference of Zeta-potential of the colloid mixed with Cu and Zn precursor. Among the test conditions, the catalyst prepared by CP at 30 °C resulted in a satisfactory dispersion characteristics in deionized water.

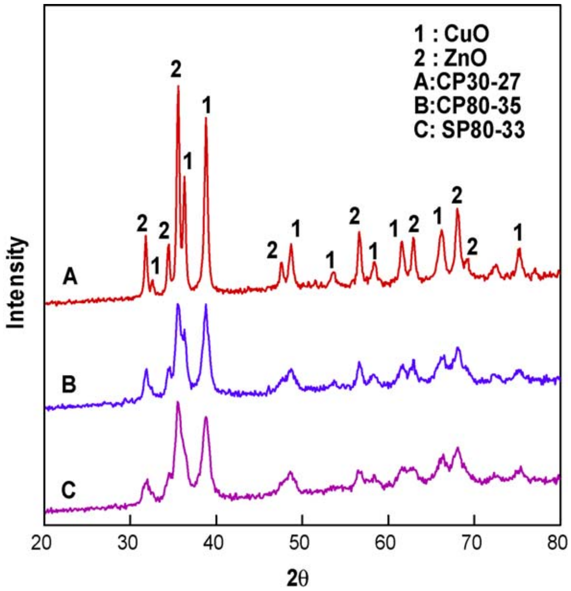

Fig. 5. XRD patterns of Cu/ZnO catalysts after calcination at 350 °C for 2 h; (A) CP at 30 °C, (B) CP at 80 °C, (C) SP at 80 °C (CP: co-precipitation, SP: sequential precipitation).

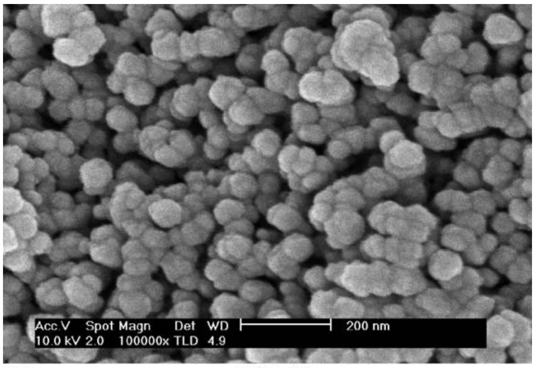

(a) CP30-27

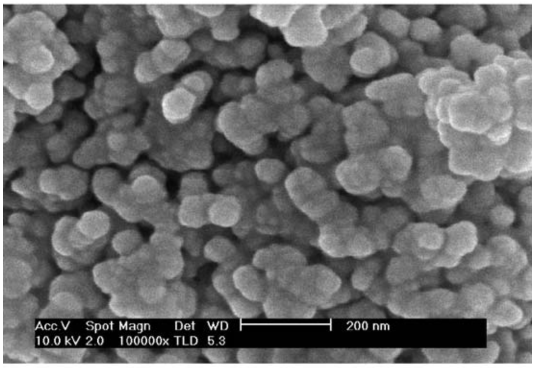

(b) CP80-35

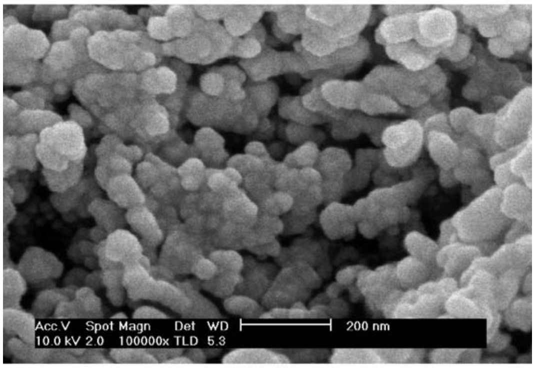

(c) SP80-33

Fig. 6. SEM images of Cu/ZnO catalysts after calcination at 350 °C for 6 h; (a) CP at 30 °C, (b) CP at 80 °C, (c) SP at 80 °C (CP: co-precipitation, SP: sequential precipitation).

6.2. Catalytic activity of Cu/ZnO catalysts

Fig. 7 is a methanol conversion performance of catalysts precipitated in different conditions. Catalyst prepared by SP at 80 °C resulted in slightly better conversion performance than other precipitation conditions. The effect of reaction temperature on the methanol conversion performance is shown in Fig. 8. In temperature higher than 250 °C, all catalysts resulted in the similar conversion performance. In temperature lower than 250 °C, however, the catalyst prepared by CP at 30 °C had the lowest conversion performance in all catalysts. This means that the catalyst prepared by CP at 30 °C has the low dispersion of Cu. This can be seen in its lower surface area as shown in Table 1.

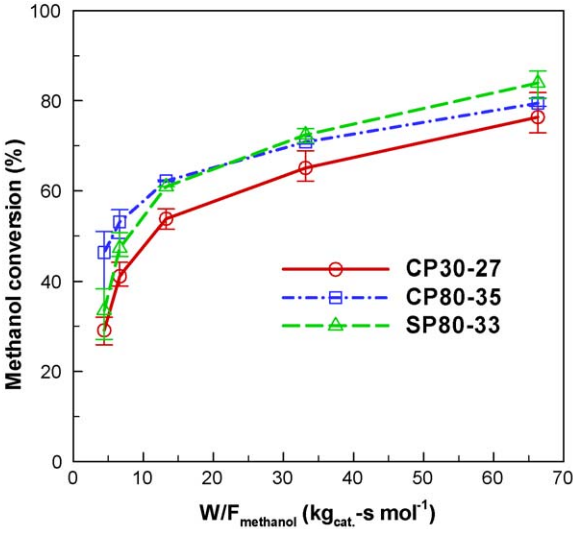

Fig. 7. Methanol conversion as a function of the space time in each catalyst at 250 °C and S/C = 1.1.

6.3. Coated catalyst layer on a wafer

Typical coating procedure can deposit 5–8 mg/cm^2 of catalysts, and the thickness of the coated layer was approximately 30 µm. Fig. 9 shows SEM images of the surface and cross-section of the catalyst-coated wafer. To obtain the required amount of the catalyst for the increased reactivity, the repetition of the coating procedure was performed. Cu/ZnO catalysts prepared in different precipitation conditions were different in the quality of repeated coating from each other. Catalyst prepared by CP at 30 °C had a crack-free and uniform surface for three times of the coating procedure. Fig. 10 is images that show the coated surface of the catalyst prepared by CP and SP at 80 °C. The surface had many cracks because the catalyst layer stripped the previous catalyst layer when the coating procedure was repeated. Fig. 11 shows the catalyst amount for the number of coated layers. By repeating the precipitating procedure of the catalyst prepared by CP at 30 °C, the catalyst amount was increased to 15 mg/cm^2. The adhesion of the catalyst coated on a wafer can be improved by controlling the precipitation time. This method can lessen a catalyst loss for the coating process compared with the spin coating and dip coating.

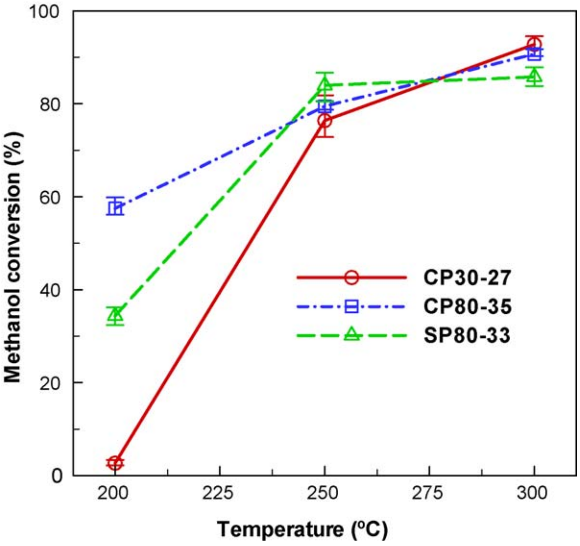

Fig. 8. Methanol conversion as a function of the temperature in each catalyst at W/F = 66.3 kg$_{cat.}$ s/mol and S/C = 1.1.

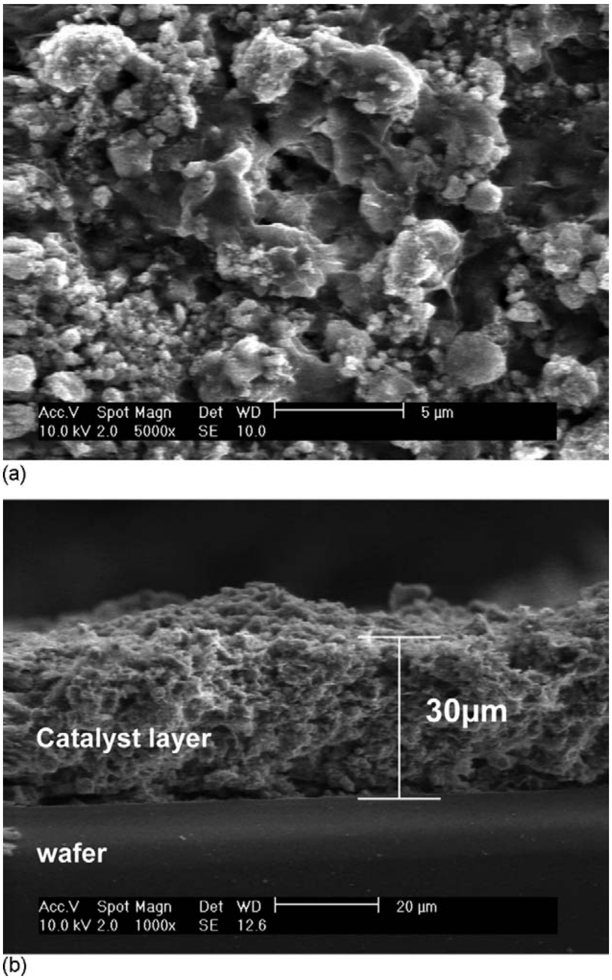

Fig. 9. SEM images of the catalyst layer coated by the precipitation method on the wafer: (a) the surface, (b) the cross-section.

6.4. Activity test of a wafer coated with Cu/ZnO catalyst

The size of the catalyst-coated wafer is 1 cm × 2 cm. For the activity test, the wafer was crashed into 10 pieces and inset the reactor (5.3 mm i.d.). From this method, the activity of the catalyst-coated wafer can be measured without the effect of resident time. Fig. 12 is a plot that shows the effect of repeated coating on the methanol conversion as a function of the feed rate at the reaction temperature of 250 °C. The methanol feed rate ranged 0.1–2 ml/h. As the thickness of the coated catalyst increased with repeated coating, the methanol conversion increased. The dependence of the methanol conversion on the feed rate diminished as the catalyst amount increase due to repeated coating. In general, the coating process itself

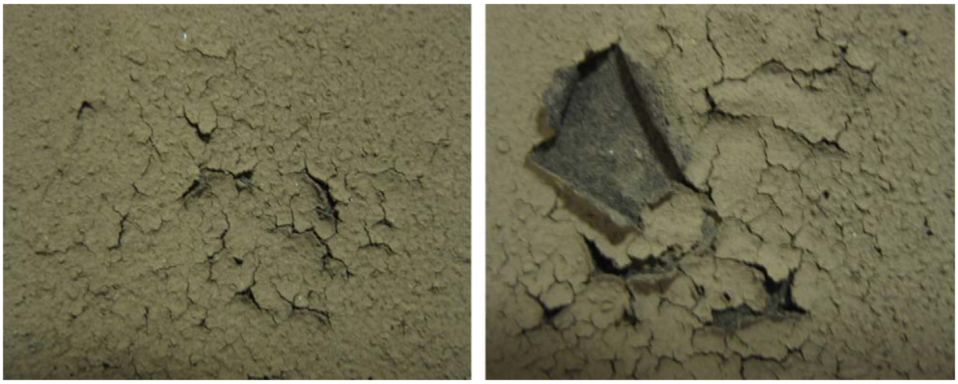

Fig. 10. Image of the coated surface of catalyst prepared by CP at 80 °C (left) and by SP at 80 °C (right).

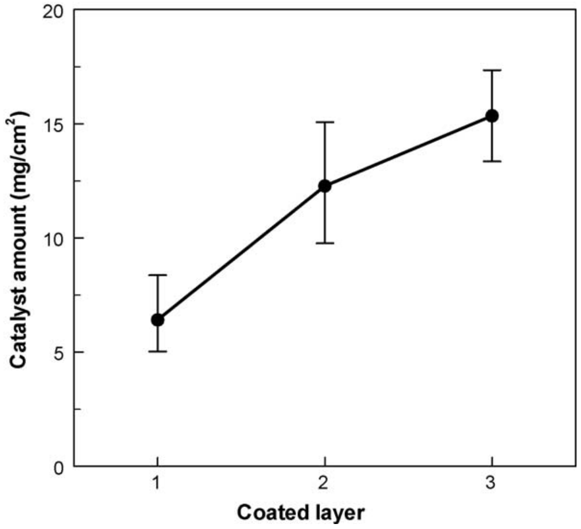

Fig. 11. The catalyst amount for the number of the coated layer.

did not seem to affect the catalyst reactivity. Fig. 13 is a result of the dependence of the methanol conversion and hydrogen production rate on the reacting temperature for the case with the feed rate of 0.1 ml/h. Like a experiment with the powder state catalyst, more than 80% of methanol was converted for the reaction temperature higher than 250 °C. These similar results demonstrate that the binder addition and the subsequent heat treatment for coating the catalyst did not affect the catalyst reactivity.

6.5. Patterned catalyst layer on a wafer

The result of catalyst patterning is presented in Fig. 14. The catalyst pattern whose width was 1 mm was obtained by the PVA lift-off process. However, micro catalyst pattern less than 1 mm width was not able to be obtained by this patterning method. When the ratio of thickness to width of the catalyst layer on the PVA layer are more than 0.03, the PVA decomposition by heating was not able to remove the catalyst layer. The advantage of this patterning process is that the sacrificial layer is removed by heating the substrate instead of etching which caused the subsequent degradation of the catalyst by the etchant exposure. This catalyst patterning process can be used to the selective coating of the catalyst in the reacting area and removing in the other parts for the fabrication of micro catalytic reactor.

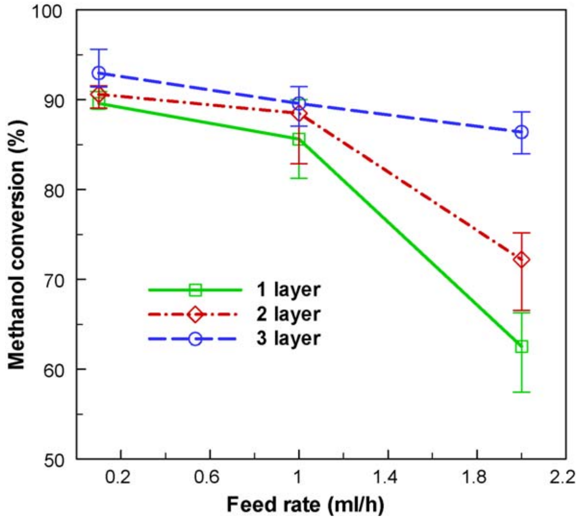

Fig. 12. Methanol conversion as a function of the feed rate in each catalyst layer at 250 °C and S/C = 1.1.

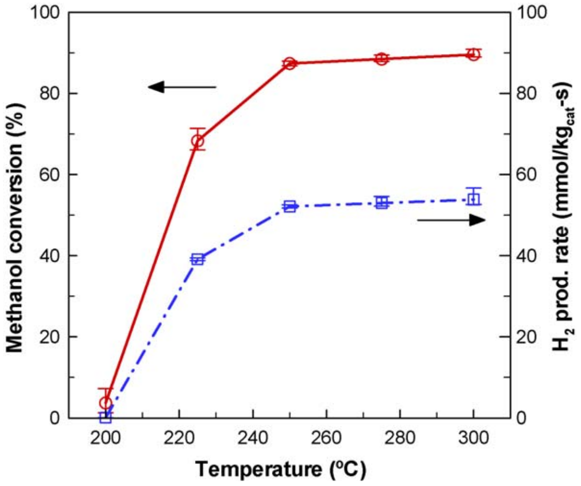

Fig. 13. Methanol conversion and hydrogen production rate as a function of the reaction temperature in the 1 layered catalyst at 0.1 ml/h and S/C = 1.1.

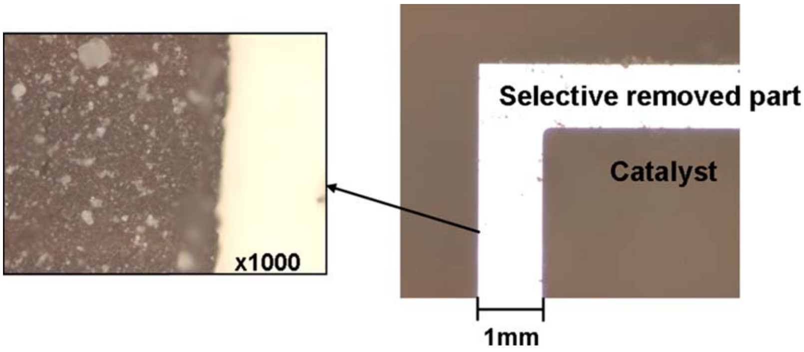

Fig. 14. Result of the catalyst patterning by the lift-off process of the PVA sacrificial layer.

6.6. *Performance measurement of the fabricated fuel reformer*

The performance of the fabricated fuel reformer was measured using the same experimental setup for the activity test of catalysts. The tubular reactor was replaced by the fabricated reformer. The feed rate of reactants was between 0.01 and 0.5 ml/h and the reaction temperature was varied from 200 to 300 °C. The catalyst was oxidized state because of the bonding process of reactor layers at the high temperature. Before tests, the catalyst was reduced by 4% H_2/N_2 mixed gas of 10 sccm at 280 °C for 4 h.

Fig. 15 shows the performance of the micro fuel reformer. Methanol conversion and hydrogen production as a function of the WHSV (weight hourly space velocity) are presented in Fig. 15(a). The WHSV is defined by the mass flow rate of methanol divided by the catalyst mass. The methanol conversion decreased as the space velocity increased. A typical methanol conversion was more than 80% to the space velocity of 22.8 h^{-1}. At 9.1 h^{-1} space velocity, the produced hydrogen per unit methanol was maximum value because the minimum carbon monoxide was produced. The effect of temperature on the micro reformer performance was shown in Fig. 15(b). The methanol conversion and the hydrogen production increased with the temperature. However, at the temperature higher than 250 °C, the hydrogen production decreased with the temperature because the production of the carbon monoxide increased. The optimum conditions are listed in Table 2. The carbon monoxide, which deactivates the anode catalyst of PEMFC, can be removed by the palladium membrane [33] and preferential oxidation [34]. In Table 2, the performance comparison of the catalyst-coated micro reformer and packed-bed reactor is presented. The micro reformer had a higher methanol conversion and hydrogen production rate than the packed-bed reactor. The microchannel, coated with the catalysts, enhanced the heat and mass transfer in a micro reformer [35] and this can be seen in its higher measured performance.

Table 2
Optimum operating conditions of the micro fuel reformer and comparison with packed-bed reactor

	Micro reformer	Packed-bed reactor
Reactor temperature (°C)	250	250
Pressure (atm)	1	1
S/C (steam to carbon ratio)	1.1	1.1
Feed flow rate (ml/h)	0.2	0.2
WHSV (h^{-1})	9.1	2.2
Methanol conversion (%)	93.1	65.1
H_2 production rate (mmol/kg s)	220.6	45.2
CO composition (%)	1.1	1.1
Inner volume of reactor (cm^3)	0.3	0.62
Catalyst amount (mg)	12	50

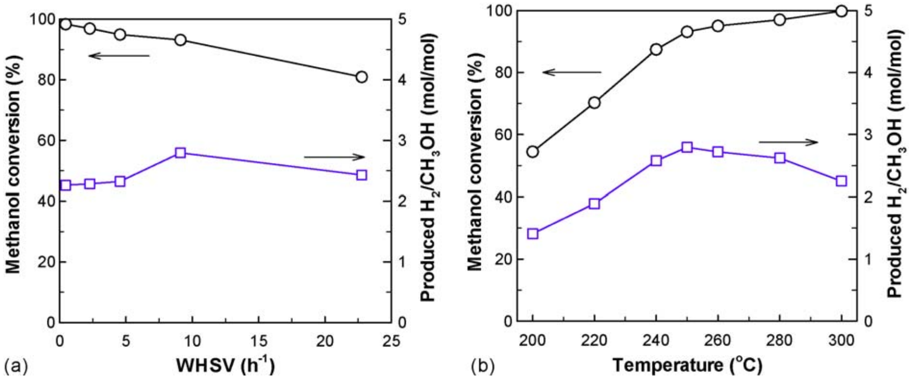

Fig. 15. Performance of the micro fuel reformer; methanol conversion and hydrogen production (a) as a function of WHSV (250 °C and S/C = 1.1), (b) as a function of temperature (WHSV = 9.1 h^{-1}, S/C = 1.1).

7. Conclusion

Catalyst preparation, coating, and patterning on a wafer are presented. The techniques were integrated into lithography procedures of a glass wafer and the complete fabrication process of a MEMS-based catalytic reactor was set up.

First, Cu/ZnO catalysts were prepared in three different conditions. The effect of temperature and sequence of precipitation on the catalyst characteristics was investigated by performing BET, XRD, SEM and activity test. It can be seen that the catalyst prepared by CP at 30 °C resulted in a good dispersion in deionized water with acceptable methanol conversion rate. Second, the coating procedure of the catalyst on a wafer was developed, resulting in the uniform and crack-free catalyst layer. By repeating the coating procedure, the catalyst amount can be controlled. From the activity test of the catalyst-coated wafer, it can be seen that the coating procedure did not affect the reactivity. Third, the novel patterning technology of the catalyst layer was attempted and then the patterned catalyst layer was obtained. PVA sacrificial layer was removed by heating instead of etching. This is an etchant-free process, preventing being exposed to the strong acid which damages the catalyst. Finally, based on the newly developed procedure, a micro fuel reformer was fabricated and its performance was evaluated.

The concept of MEMS-based catalytic reactor was demonstrated. The coating and patterning of the catalyst on a wafer proposed in the present study would be utilized for developing various micro catalytic reactors.

Acknowledgements

This work is supported by the NANOFINE program funded by the Ministry of Commerce, Industry, and Energy. Their support is gratefully acknowledged.

References

[1] J.D. Holladay, J.S. Wainright, E.O. Jones, S.R. Gano, Power generation using a mesoscale fuel cell integrated with a microscale fuel processor, J. Power Sources 130 (2004) 111–118.

[2] J.P. Meyers1, H.L. Maynard, Design considerations for miniaturized PEM fuel cells, J. Power Sources 109 (2002) 76–88.

[3] K. Shah, W.C. Shin, R.S. Besser, A PDMS micro proton exchange membrane fuel cell by conventional and non-conventional microfabrication techniques, Sensors Actuators B97 (2004) 157–167.

[4] J.D. Morse, A.F. Jankowski, R.T. Graff, J.P. Hayes, Novel proton exchange membrane thin-film fuel cell for micro-scale energy conversion, J. Vac. Sci. Technol. A 18 (4) (2000) 2003–2005.

[5] K.-B. Min, S. Tanaka, M. Esashi, MEMS-based polymer electrolyte fuel cell, Electrochemistry 70 (12) (2002) 924–927.

[6] K.-B. Min, S. Tanaka, M. Esashi, Silicon-based micro-polymer electrolyte fuel cells, in: Proc. of the IEEE 16th Annual Int. Conf. on Microelectromech. Syst., Kyoto, Japan, 2003, pp. 379–382.

[7] S.J. Lee, A. Chang-Chien, S.W. Cha, R. O'Hayre, Y.I. Park, Y. Saito, F.B. Prinz, Design and fabrication of a micro fuel cell array with "flip-flop" interconnection, J. Power Sources 112 (2) (2002) 410–418.

[8] T.J. Yen, N. Fang, X. Zhang, G.Q. Lu, C.Y. Wang, A micro methanol fuel cell operating at near room temperature, Appl. Phys. letters 83 (19) (2003) 4056–4058.

[9] G.Q. Lu, C.Y. Wang, T.J. Yen, X. Zhang, Development and characterization of a silicon-based micro direct methanol fuel cell, Electrochimica Acta 49 (5) (2004) 821–828.

[10] Y. Sim, G.Y. Kim, S.S. Yang, Fabrication of micro power source using a micro direct methanol fuel cell for the medical applications, in: Proc. of the IEEE 14th Annual Int. Conf. on Microelectromech. Syst., 2001, pp. 341–344.

[11] M. Mench, Z.H. Wang, K. Bhatia, C.Y. Wang, Design of a micro direct methanol fuel cell, in: Proc. of Int. Mech. Eng. Cong. and Expo., New York, USA, 2001.

[12] V. Gogel, T. Frey, Zhu Yongsheng, K.A. Friedrich, L. Jörissen, J. Garche, Performance and methanol permeation of direct methanol fuel cells: dependence on operating conditions and on electrode structure, J. Power Sources 127 (2004) 172–180.

[13] Shuji Tanaka, Kuei-Sung Changa, Kyong-Bok Mina, Daisuke Satoh, Kazushi Yoshida, Masayoshi Esashi, MEMS-based components of a miniature fuel cell/fuel reformer system, Chem. Eng. J. 101 (2004) 143–149.

[14] D.R. Jamie, J.D. Holladay, Development of a soldier-portable fuel cell power system Part 1: A bread-board methanol fuel processor, J. Power Sources 108 (2002) 28–34.

[15] J.D. Holladay, E.O. Jones, Microfuel processor for use in a miniature power supply, J. Power Sources 108 (2002) 21–27.

[16] G.G. Park, D.J. Seo, S.H. Park, Y.G. Yoon, C.S. Kim, W.L. Yoon, Development of microchannel methanol steam reformer, Chem. Eng. J. 101 (2004) 87–92.

[17] Shin-Kun Ryi, Jong-Soo Park, Seung-Hoon Choi, Sung-Ho Choa, Sung-Hyun, Novel micro fuel processor for PEMFCs with heat generation by catalytic combustion, Chem. Eng. J. 113 (2005) 47–53.

[18] G.-G. Park, S.-D. Yim, Y.-G. Yoon, C.-S. Kim, D.-J. Seo, K. Eguchi, Hydrogen production with integrated microchannel fuel processor using methanol for portable fuel cell systems, Catal. Today 110 (2005) 108–113.

[19] A.V. Pattekar, M.V. Kothare, A microreactor for hydrogen production in micro fuel cell applications, J. Microelectromech. Syst. 13 (1) (2004) 7–18.

[20] L.R. Arana, S.B. Schaevitz, A.J. Franz, M.A. Schmidt, K.F. Jensen, A microfabricated suspended-tube chemical reactor for thermally efficient fuel processing, J. Microelectromech. Syst. 12 (5) (2003) 600–612.

[21] B. Lindstrom, L.J. Pettersson, Development of a methanol fuelled reformer for fuel cell applications, J. Power Sources 118 (2003) 71–78.

[22] B. Hohlein, M. Bee, J. Bogild-Hansen, P. Brockerhoff, G. Colsman, B. Emonts, R. Menzer, E. Riedel, Hydrogen from methanol for fuel cells in mobile systems: development of a compact reformer, J. Power Sources 61 (1996) 143–147.

[23] S.T. Yong, K. Hidajat, S. Kawi, Reaction of auto thermal steam reforming of methanol to hydrogen using a novel nano CuZnAl-catalyst, J. Power Sources 131 (2004) 91–95.

[24] Zhigang Qi, Chunzhi He, Arthur Kaufman, Effect of CO in the anode fuel on the performance of PEM fuel cell cathode, J. Power Sources 111 (2002) 239–247.

[25] J. Agrell, M. Boutonnet, I. Melian-Cabrera, Jose L.G. Fierro, Production of hydrogen from methanol over binary Cu/ZnO catalysts, Part 1. Catalyst preparation and characterization, Appl. Catal. A Gen. 253 (1998) 201–211.

[26] John P. Breen, Julian R.H. Ross, Methanol reforming for fuel-cell applications: development of zirconia-containing Cu-Zn-Al catalysts, Catal. Today 51 (1999) 521–533.

[27] J. Bravo, A. Karim, T. Conant, G.P. Lopez, A. Datye, Wall coating of a CuO/ZnO/Al_2O_3 methanol steam reforming catalyst for micro-channel reformers, Chem. Eng. J. 101 (2004) 113–121.

[28] D.H. Lee, Measurement and analysis of thermochemical process for micro power generation, Ph.D. Thesis, KAIST, 2003 pp. 89–90.

[29] J. Agrell, H. Birgersson, M. Boutonnet, Steam reforming of methanol over a Cu/ZnO/Al_2O_3 catalyst: a kinetic analysis and strategies for suppression of CO formation, J. Power Sources 106 (2002) 249–257.

[30] B.A. Peppley, J.C. Amphett, L.M. Kearns, R.F. Mann, Methanol steam reforming on Cu/ZnO/Al_2O_3 catalysts, Part 2. A comprehensive kinetic model, Appl. Catal. A Gen. 179 (1999) 31–50.

[31] T.R. Dietrich, W. Ehrfeld, M. Lacher, M. Kramer, B. Speit, Fabrication technologies for Microsystems utilizing photoetchable glass, Microelectro. Eng. 30 (1996) 497–504.

[32] Y.-R. Cho, J.-Y. Oh, H.-S. Kim, H.-S. Jeong, Micro-etching technology of high aspect ratio frameworks for electronic devices, Mater. Sci. Eng. B 64 (1999) 79–83.

[33] H.D. Tong, J.W. E. Berenschot, M.J. De Boer, J.G.E. Gardeniers (Han), W. Henk, H.V. Jansen, W. Nijdam, M.C. Elwenspoek, F.C. Gielens (Frank), C.J.M. van Rijn, Microfabrication of palladium–silver alloy membranes for hydrogen separation, J. Microelectromech. Syst. 12 (5) (2003) 622–629.

[34] E.R. Delsman, M.H.J.M. De Croon, A. Pierik, G.J. Kramer, P.D. Cobden, Ch. Hofmann, V. Cominos, J.C. Schouten, Design and operation of a preferential oxidation microdevice for a portable fuel processor, Chem. Eng. Sci. 59 (2004) 4795–4802.

[35] A. Karim, J. Bravo, D. Gorm, T. Conant, A. Datye, Comparison of wall-coated and packed-bed reactors for steam reforming of methanol, Catal. Today 110 (2005) 86–91.